Luminescent properties of novel red-emitting phosphor: Gd2O2CN2:Eu3+

Luting Wang, Shuanglong Yuan, Yunxia Yang, François Cheviré, Franck Tessier, Guorong Chen

▶ **To cite this version:**

Luting Wang, Shuanglong Yuan, Yunxia Yang, François Cheviré, Franck Tessier, et al.. Luminescent properties of novel red-emitting phosphor: Gd2O2CN2:Eu3+. Optical Materials Express, 2015, 5 (11), pp.2626-2624. 10.1364/OME.5.002616 . hal-01218122

HAL Id: hal-01218122
https://hal.science/hal-01218122

Submitted on 28 Oct 2015

HAL is a multi-disciplinary open access archive for the deposit and dissemination of scientific research documents, whether they are published or not. The documents may come from teaching and research institutions in France or abroad, or from public or private research centers.

L'archive ouverte pluridisciplinaire **HAL**, est destinée au dépôt et à la diffusion de documents scientifiques de niveau recherche, publiés ou non, émanant des établissements d'enseignement et de recherche français ou étrangers, des laboratoires publics ou privés.

Luminescent properties of novel red-emitting phosphor: $Gd_2O_2CN_2:Eu^{3+}$

Luting Wang[1]，Shuanglong Yuan[1,3]，Yunxia Yang[1]，Francois Chevire[2,4]，Franck Tessier[2], Guorong Chen[1]

1. Key Laboratory for Ultrafine Materials of Ministry of Education, School of Materials Science and Engineering, East China University of Science and Technology, Shanghai 200237, China

[2]Institut des Sciences Chimiques de Rennes (UMR CNRS 6226), équipe Verres et Céramiques, Université de Rennes 1, F-35042 Rennes cedex, France

[3]*Shuanglong@ecust.edu.cn*

[4]*Francois.Chevire@univ-rennes1.fr*

Abstract: Eu^{3+}-doped $Gd_2O_2CN_2$ was firstly synthesized by a classical solid-state reaction of Li_2CO_3, Eu_2O_3 and GdF_3 under NH_3 gas flow in the presence of graphite at low firing temperature. Powder X-ray diffraction (XRD) analysis indicated that $Gd_2O_2CN_2$: Eu^{3+} crystallizes in a trigonal-type structure with space group P-3m1. $Gd_2O_2CN_2$: Eu^{3+} shows a sharp red emission band peaking at 626 nm under excitation at 300 nm at room temperature. PL spectra indicates that Eu^{3+} doped $Gd_2O_2CN_2$ samples emit the typical emission peaks at 614 nm and 626 nm originated from the hypersensitive electric dipole transition ($^5D_0 \rightarrow {}^7F_2$) of Eu^{3+} ions. The optimized doping concentration of Eu^{3+} ions was found to be 7.5 at.%, and the critical transfer distance was calculated to be 10.907 Å.

1. Introduction:

Recently, much attention has been paid on investigating red emitting phosphors owing to their potential applications in X-ray mammography [1], in display devices [2-3] and especially in white light emitting diodes (WLEDs) [4-6]. Eu^{3+}- doped luminescent materials as the main and outstanding red-emitting phosphors, such as Eu^{3+} doped Y_2O_3 [3], Y_2O_2S [7], $R_2(MoO_4)_3$ (R=La, Y, Gd)[8] and $NaEu(WO_4)_2$[5], have been studied for decades due to the transition of $^5D_0$-^7F_J (J = 1-6) of Eu^{3+}. However, these excellent red emitting phosphors can hardly fulfill the demands for novel high-performance

materials. Therefore, the exploration of novel luminescent host materials remains a meaningful work.

The crystal structures of rare earth oxysulfides RE_2O_2S and oxycyanamides $RE_2O_2CN_2$ are closely related [9] and consist of $RE_2O_2^{2+}$ layers and their interleaving anions. Eu^{3+} doped RE_2O_2S has been widely used as phosphor for CRT [10]. The luminescence properties of $Y_2O_2CN_2$: Eu^{3+} are quite similar to those of the commercially used red emitter Y_2O_2S: Eu^{3+} [9]. Therefore, oxycyanamide compounds are considered to be efficient host candidates for good luminescence performance. Rare earth dioxymonocyanamides ($RE_2O_2CN_2$, RE=La, Ce, Pr, Nd, Sm, Eu, Gd)[11] were prepared by nitriding a mixture of rare earth oxide in flowing ammonia at 950 °C. The luminescent properties of $RE_2O_2CN_2$:M^{3+} (Ln = Y, Gd and La, M^{3+} = Tb^{3+}, Eu^{3+}, Pr^{3+}, Er^{3+} and Er^{3+}/Tb^{3+}) have been previously studied[11-14]. Eu^{3+} doped $Gd_2O_2CN_2$ was firstly prepared by sol-gel method by Takeda et al., but the luminescence intensity was weak because of its low crystallinity and the suppression of concentration quenching was not recognized because of the presence of impurities for high Eu-doping concentration [15]. Thus, we propose here to further investigate the preparation and photoluminescence properties of pure micrometric $Gd_2O_2CN_2$:Eu^{3+} phosphors.

In this paper, a series of Eu^{3+} doped $Gd_2O_2CN_2$ samples with 1-3 μm particle size were successfully prepared for the first time by a classic solid state route using GdF_3, Li_2CO_3 and Eu_2O_3 as raw material. The phase structures of the samples were determined by powder X-ray diffraction (XRD). Luminescence properties and the concentration quenching characteristics were also investigated in detail.

2. Experimental:

Powder samples with the general formula $(Gd_{1-x}Eu_x)_2O_2CN_2$ [x=0.005(GOCN-1), 0.02(GOCN-2), 0.035(GOCN-3), 0.05(GOCN-4), 0.075(GOCN-5) and 0.10 (GOCN-6)] were prepared starting from high purity GdF_3 (99.99%), Eu_2O_3 (99.99%), Li_2CO_3 (99.99%), and active carbon (CARBIO 12 SA—ref: C1220 G 90) as raw materials. All starting materials were weighted in the proper stoichiometries, and finely mixed in an agate mortar. The mixture was placed at the end of a graphite boat,

while active carbon was put in the upcoming flowing gas at the other end. After that, the mixture was fired at 600 °C for 9 h, then 750 °C for 12 h and finally cooled down to room temperature under NH_3 atmosphere in a tubular furnace. The sintered samples were further washed with distilled water to remove LiF by-products (determined by XRD) from the reaction product and dried at 120 °C in air. Finally, the as-prepared fine powders were collected for characterization.

$$2(1\text{-}x)GdF_3 + xEu_2O_3 + 3(1\text{-}x)Li_2CO_3 + C + 2NH_3 \rightarrow$$
$$(Gd_{1-x}Eu_x)_2O_2CN_2 + 6(1\text{-}x)LiF + 3(1\text{-}x)CO_2 + H_2O + 2H_2$$

Powder X-ray diffraction (XRD) data were recorded using a Bruker AXS D8 Advance diffractometer (Voltage 50 kV, current 40 mA, Cu-Ka) with a step width of 0.02. Photoluminescence (PL) and photoluminescence excitation (PLE) spectra were measured by a Fluorolog-3-P UV-vis-NIR fluorescence spectrophotometer (Jobin Yvon, longjumeau, France) with a 450 W Xenon lamp as the excitation source. The surface morphology and particles size of the phosphor samples were examined by a field emission scanning electron microscope (FE-SEM, S-4800, Hitachi High-Technologies) with high voltage of 15 kV. The BET-specific surface area was measured by ASAP 2460 surface area and porosity analyzer made by Micromeritics Instrument Corporation. The FTIR spectrum was measured in transmission mode using a KBr standard (Bruker, Model vector 22). The color chromaticity coordinates were obtained according to Commission Internationale de I'Eclairage (CIE) using Radiant Imaging color calculator software. All spectroscopic measurements were carried out at room temperature.

3. Results and Discussion

$Eu_2O_2CN_2$ and $Gd_2O_2CN_2$ have the same crystal structure based on a trigonal unit cell with the space group P-3m1 and the linear CN_2^{2-} ions lay perpendicular to $RE_2O_2^{2+}$ (RE=Eu and Gd) layers [11]. The $Eu^{3+}$and Gd^{3+} ions are both coordinated with four oxygen and three nitrogen atoms in a seven-fold coordination with the oxygen and the metal in the same plane. Thus, Eu^{3+} ions can partially substitute for Gd^{3+} ions to form a $(Gd_{1-x}Eu_x)_2O_2CN_2$ (x=0.005-0.10) solid solution as illustrated by XRD patterns presented in Fig. 1. The characteristic diffraction peaks of all samples can be

ascribed to the trigonal structure of $Gd_2O_2CN_2$ (PDF#49-1169) with the space group P-3m1. No other impurity phase can be detected at the current doping concentrations. With the increase of Eu^{3+}-doping concentration, the diffraction peaks of the samples slightly shift to lower diffraction angles compared with those of $Gd_2O_2CN_2$ (PDF#49-1169), as shown in the second part of Fig. 1. The shift of diffraction angles can be attributed to the replacement of the smaller Gd^{3+} (r = 0.100 nm) by relatively larger Eu^{3+} (r = 0.101 nm), indicating a compacter lattice configuration. Meanwhile, the Eu^{3+} doping limit has been increased to 10 at. % compared to 4 at. % previously reported in sol-gel synthesis [15].

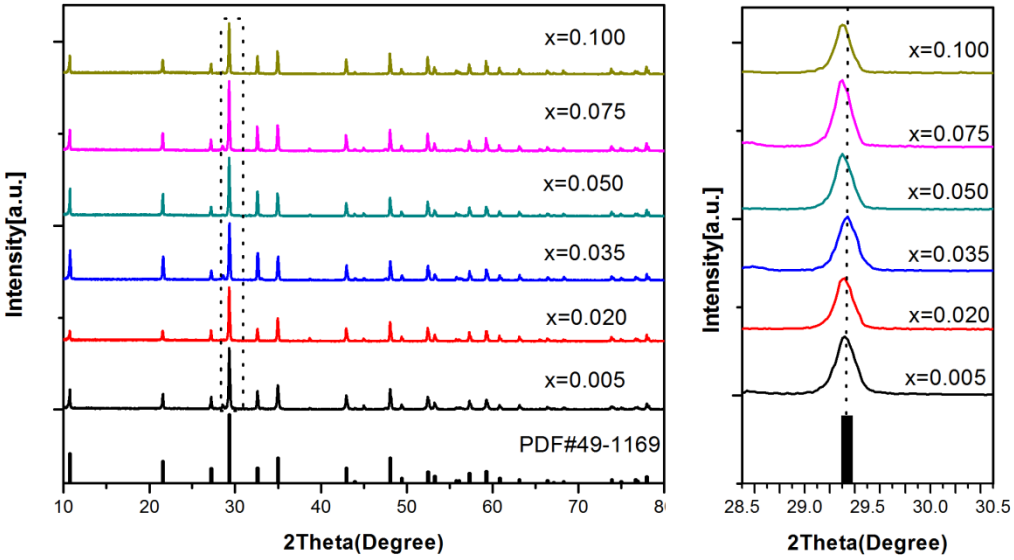

Fig.1. XRD patterns of $(Gd_{1-x}Eu_x)_2O_2CN_2$ (x=0.005, 0.02, 0.035, 0.050, 0.075, 0.100) with PDF standard card of $Gd_2O_2CN_2$.

Figure 2 shows the IR spectra of $Gd_2O_2CN_2:Eu^{3+}$ samples with different concentration of Eu^{3+}. All IR spectra samples show two typical absorption peaks in the vicinity of 652 and 2100 cm^{-1}. These absorption peaks ca. 652 and 2100 cm^{-1} were assigned to the ν_2 (bending vibration) and ν_3 (asymmetric stretching vibration) modes of the CN_2^{2-} ion which were comparable to the IR spectrum of $RE_2O_2CN_2$ [16, 17] (RE= Ce, Pr, Nd, Sm, Eu, Gd), indicating the presence of CN_2^{2-} ions in the $Gd_2O_2CN_2:Eu^{3+}$ samples. The other peaks around 400-500cm^{-1} have not been assigned as yet.

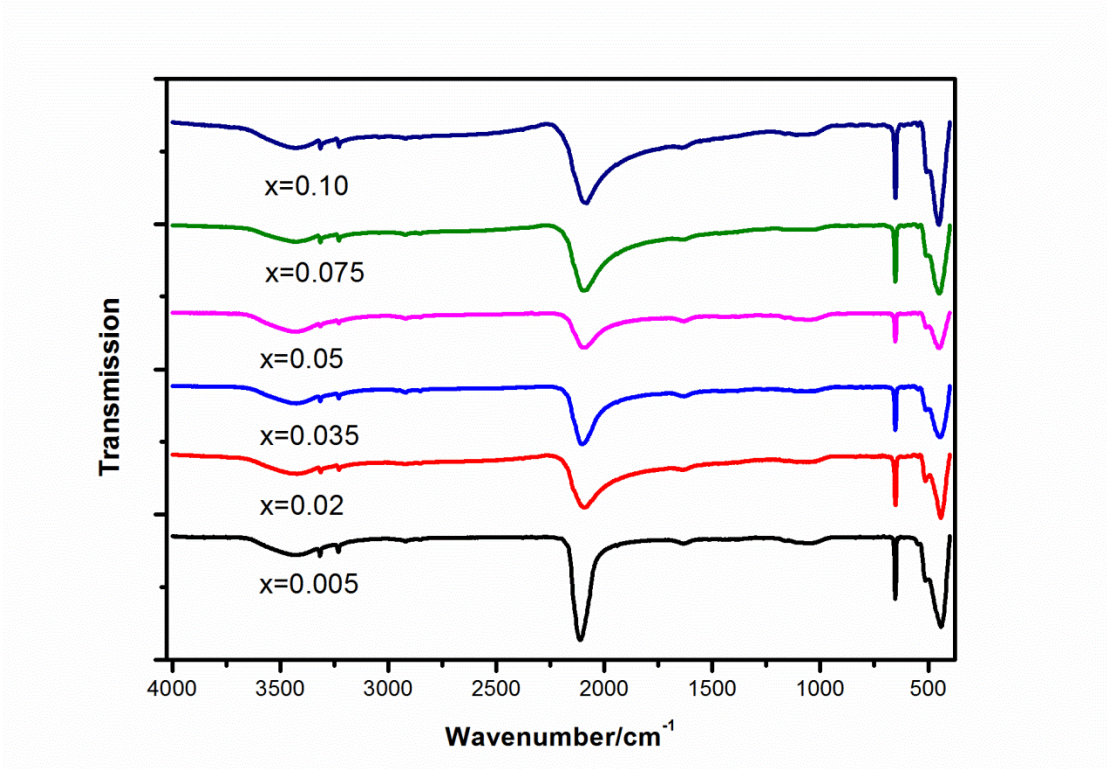

Fig.2. IR spectra of $(Gd_{1-x}Eu_x)_2O_2CN_2$ (x=0.005, 0.02, 0.035, 0.05, 0.075, 0.10) samples

Figure 3 displays SEM images of GOCN-6, GOCN-4 and GOCN-5 samples. It can be noticed that the prepared samples with various Eu^{3+} concentrations exhibit similar morphology and particles size ranging from 1 to 3 μm. Meanwhile, the specific surface area of GOCN-4 is determined to be 0.64 m^2/g.

The elementary composition of GOCN-4 is further confirmed by energy dispersive X-ray spectrometry (EDS), as shows in Fig. 4. The energy dispersive spectrum reveals the presence of Gd, O, N and C elements and allows estimating the composition for the host matrix elements as Gd atom% = 27.32%, O at. % = 25.3 %, N at. % = 22.95 % and C at. % = 24.43 % which are in rough agreement with the formula of host matrix $Gd_2O_2CN_2$ except for the C at. %. The overestimation of the carbon content comes the conductive adhesive used for preparation sample for EDS analyses.

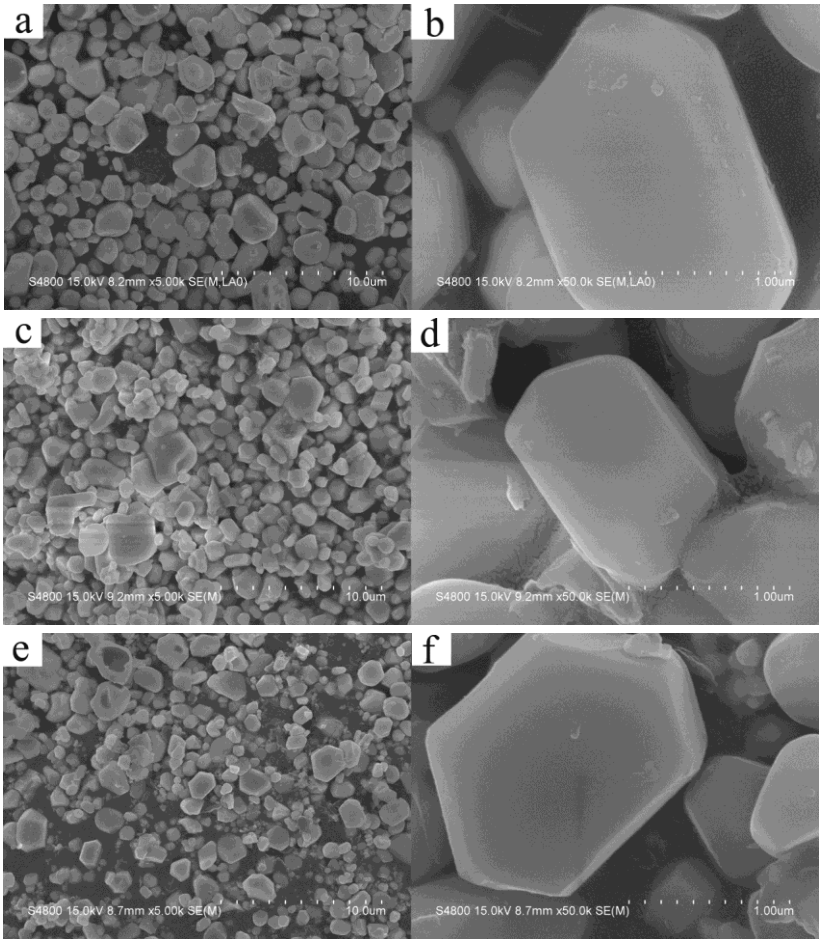

Fig.3. (Left) SEM image of $Gd_{1.80}Eu_{0.2}O_2CN_2$(a), $Gd_{1.90}Eu_{0.1}O_2CN_2$ (c) and $Gd_{1.85}Eu_{0.15}O_2CN_2$ (e) at low-magnification (5.00K). (Right) SEM image of $Gd_{1.80}Eu_{0.2}O_2CN_2$ (b), $Gd_{1.90}Eu_{0.1}O_2CN_2$ (d) and $Gd_{1.85}Eu_{0.15}O_2CN_2$ (f) at high-magnification (50.0K).

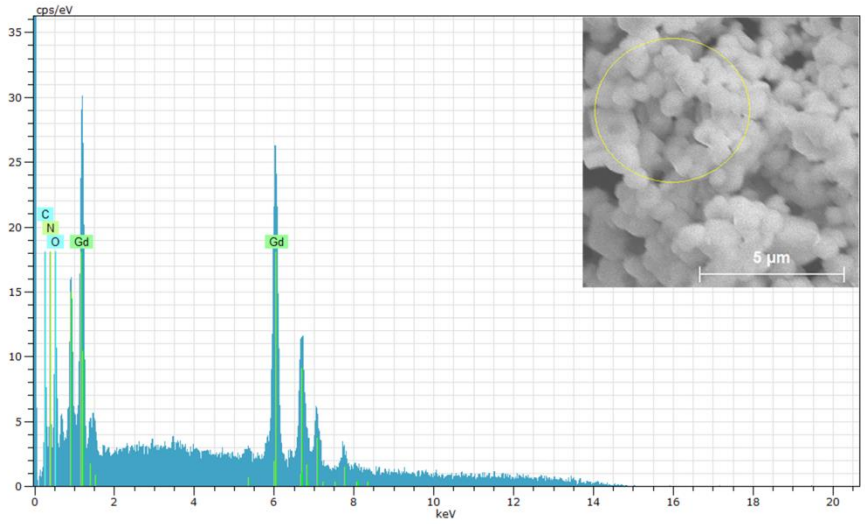

Fig.4. EDS spectra of $Gd_{1.90}Eu_{0.1}O_2CN_2$ sample

Figure 5 illustrates the excitation (monitored by 626 and 614 nm) and emission (excited by 300, 395 and 467 nm) spectra of the GOCN-5 sample. The excitation spectra (Fig. 5a) exhibit a broad and intense band in the range from 250 to 350 nm with a maximum located at around 300 nm. This band is attributed to the ligand-to-metal charge transfer between O^{2-} and Eu^{3+}, the CTB (Charge-transfer band) of GOCN-5 corresponds to the electron transition from the 2p orbital of O^{2-} to the 4f orbital of Eu^{3+} [18]. The weak excitation bands at lower energy, i.e. at longer wavelengths, correspond to the expected 4f-4f transitions within the $[Xe]4f^6$ configuration of Eu^{3+} and are located at 362 nm ($^7F_1 \rightarrow {}^5G_3$), 384 nm ($^7F_0 \rightarrow {}^5G_2$),395 nm ($^7F_0 \rightarrow {}^5L_6$), 417 nm ($^7F_0 \rightarrow {}^5D_3$) and 467 nm ($^7F_0 \rightarrow {}^5D_2$).

The emission spectra of GOCN-5 (Fig. 5b) at different excitation wavelengths are very similar both in shape and relative intensities. The strongest peak splits into two peaks at 614 and 626 nm which originates from the electric dipole transition $^5D_0 \rightarrow {}^7F_2$ of Eu^{3+}, indicating that Eu^{3+} occupies a site with no inversion center low symmetry in GOCN-5 [19]. This transition is sensitive to crystal-structure and chemical surroundings. According to previous studies, the dominated emission of Y_2O_3:Eu^{3+} is located at 613 nm [20] and $Y_2O_2CN_2$:Eu^{3+} shows red luminescence at 614 nm and 626.5 nm [9] which are both due to the $^5D_0 \rightarrow {}^7F_2$ transition within europium. Meanwhile, the emitted radiation of Gd_2O_3:Eu^{3+} is dominated by the red emission peak at 612 nm [21]. From the predominant peaks at 614 and 626 nm, it can be further proved the formation of the oxycyanamide host [13-15]. Some weak peaks can be observed at 580 nm, 590 nm, 594 nm and 653 nm, corresponding to the forbidden transition $^5D_0 \rightarrow {}^7F_0$ (580 nm) and the magnetic dipole transitions $^5D_0 \rightarrow {}^7F_1$ (590 nm and 594 nm) and $^5D_0 \rightarrow {}^7F_3$ (653 nm).

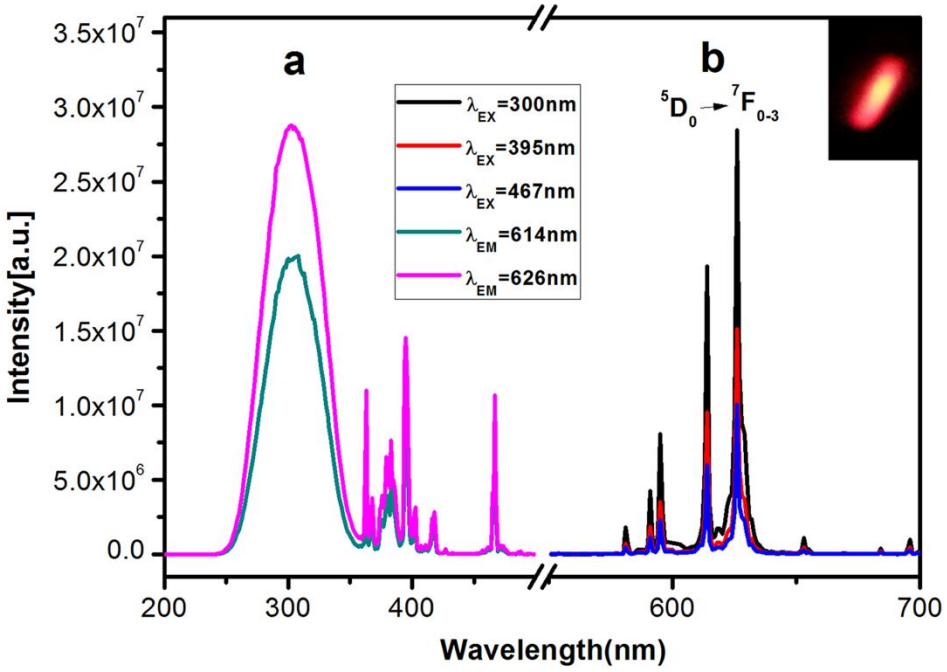

Fig.5. Excitation (a) and Emission (b) spectra of the $Gd_{1.85}Eu_{0.15}O_2CN_2$ sample. The right inset is the photograph image of the Eu^{3+}-doped sample being excited by the 300 nm lights.

Fig. 6 shows the PL and PLE spectra of $Gd_2O_2CN_2$: Eu^{3+} samples with various concentrations of Eu^{3+} ions. While the spectral shape and locations of excitation and emission peaks do not vary with the doping concentration of Eu^{3+} ions, the photoluminescence intensity strongly depends on it. With the increase of doped Eu^{3+} ions concentration, the excitation and the emission intensity increases gradually ranging from 0.5 to 7.5 at. % and decreases from 7.5 to 10 at. %. Thus the optimized Eu^{3+} ions doping concentration in $Gd_2O_2CN_2$ host matrix is about 7.5 at. %. Considering the mechanism of energy transfer in phosphors, the concentration quenching can be explained in more detail by the critical distance (R_c) between Eu^{3+} ions which can be calculated by the following formula [22]:

$$R_c = 2 \times (3V/4\pi X_c N)^{1/3} \qquad (2)$$

Where V is the volume of the unit cell, X_c is the critical concentration of Eu^{3+} ions and N is the number of lattice sites in the unit cells that can be occupied by Eu^{3+} ions. For the $Gd_2O_2CN_2$ host, V=101.9 $Å^3$, X_c =0.075 and N=2. Therefore, the average distances R_c between Eu^{3+} ions is calculated to be R_c=10.907 Å when the optimized doping molar concentration is 7.5 at. %.

It is interesting to note that the optimized Eu^{3+} concentration in $Gd_2O_2CN_2$ host

matrix (7.5 at. %) is higher than that in Gd_2O_2S and Gd_2O_3 host matrix that is around 5 at% [23]. The suppression of concentration quenching is attributed to the two-dimensional character of the $Gd_2O_2CN_2$ structure. The trigonal structure of $Gd_2O_2CN_2$ consists of $Gd_2O_2^{2+}$ and CN_2^{2-} layers. The $Gd_2O_2^{2+}$ layers are perpendicular to the c axis and the linear CN_2^{2-} ions are parallel to the c axis [11]. This kind of structure leads to a long interlayer distance between the $Gd_2O_2^{2+}$ slabs (≈0.57 nm) which contributes to the higher doping concentration of Eu^{3+}[15].

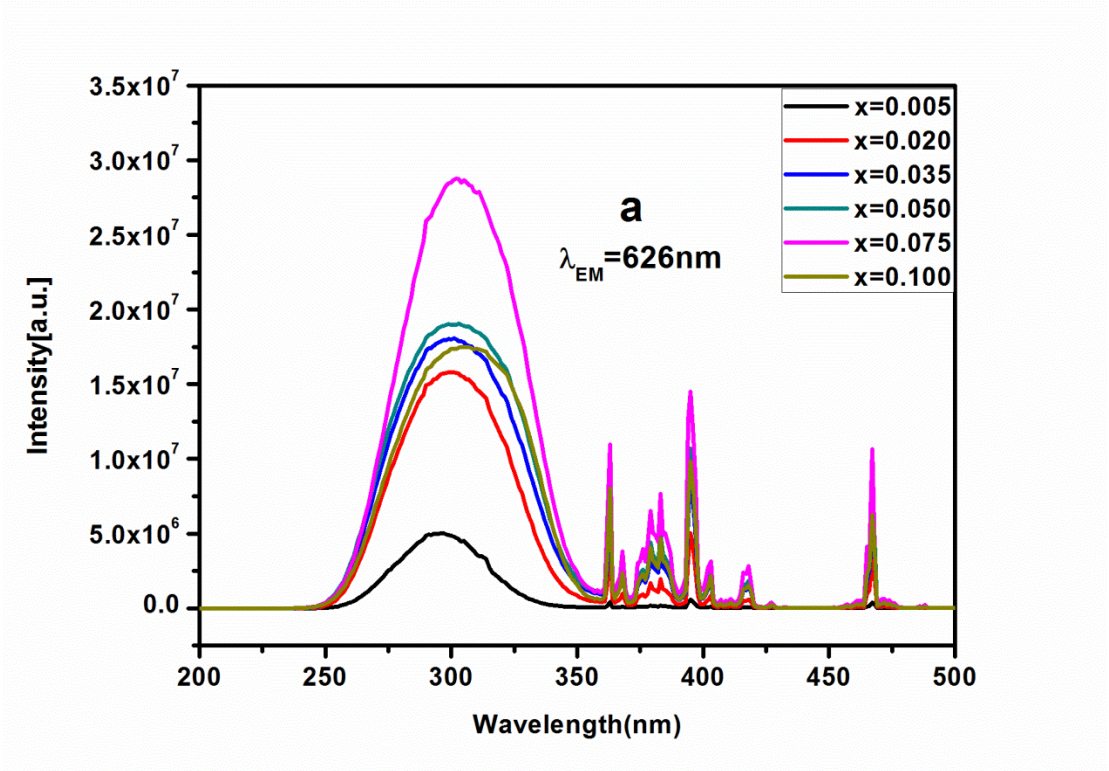

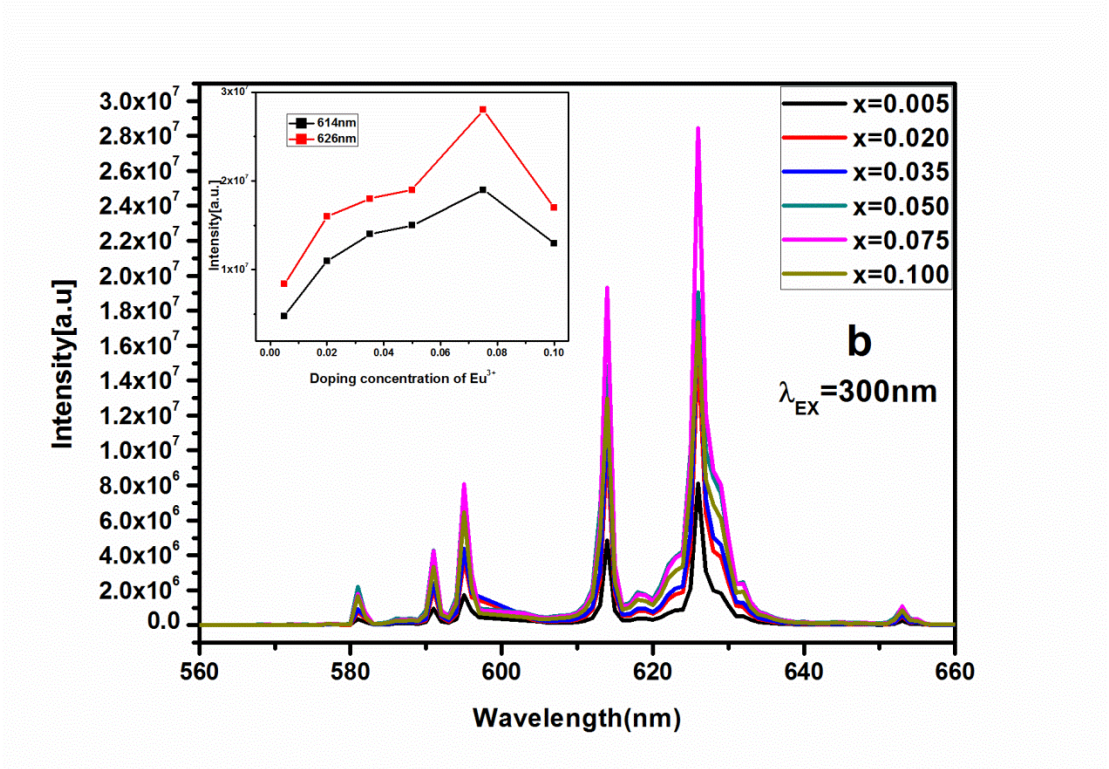

Fig.6. Excitation (a) and emission (b) spectra of $(Gd_{1-x}Eu_x)_2O_2CN_2$ (x=0.005, 0.02, 0.035, 0.05, 0.075, 0.100) samples. The inset is the dependence of its PL intensity on the Eu^{3+} content in the $Gd_2O_2CN_2$ matrix.

The color chromaticity coordinates have been calculated for the optimized sample $Gd_{1.85}Eu_{0.15}O_2CN_2$ under a 467 nm excitation (Fig. 7). The calculated values (0.6475, 0.3488) are very close to the CIE color coordinates of the red region, indicating $Gd_{1.85}Eu_{0.15}O_2CN_2$ phosphor is a promising red emitting phosphor for WLEDs application.

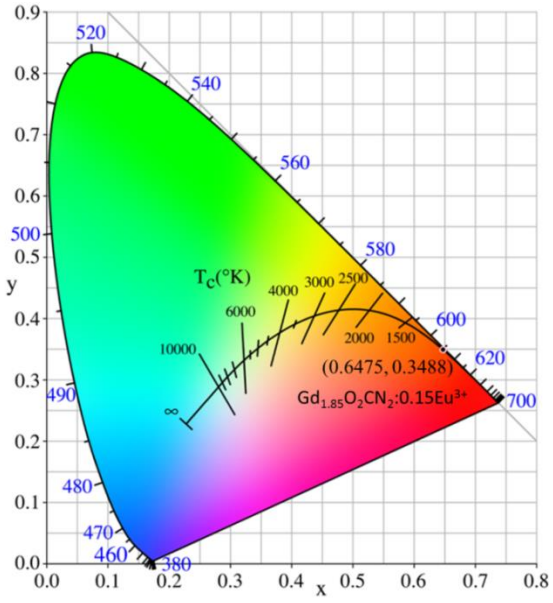

Fig.7. The 1931 CIE chromaticity coordinate for $Gd_{1.85}Eu_{0.15}O_2CN_2$under 467nm excitation.

4. Conclusion

In this paper, pure phase $(Gd_{1-x}Eu_x)_2O_2CN_2$(x=0.005, 0.02, 0.035, 0.050, 0.075, 0.100) phosphors with space group P-3m1 have been prepared using GdF_3, Li_2CO_3 and Eu_2O_3 as raw materials at low firing temperature (750 °C), for the first time. The Eu^{3+} doped $Gd_2O_2CN_2$ phosphors exhibit a characteristic red emission. The strongest and second strongest peaks are located at 626 and 614 nm ($^5D_0 \rightarrow {}^7F_2$ transition) under excitation of 300, 395 and 467 nm. The strongest luminescent intensity of $Gd_2O_2CN_2$:Eu^{3+} is obtained when the doping concentration of Eu^{3+} reaches 7.5 at. %. The optimized Eu^{3+} doping concentration in $Gd_2O_2CN_2$ is higher than that in Gd_2O_3 and Gd_2O_2S host lattices, which is due to the 2D structure of the $Gd_2O_2CN_2$ host matrix. The CIE chromaticity coordinates (0.6475, 0.3488) for $Gd_{1.85}Eu_{0.15}O_2CN_2$ phosphor are located in the red region. All the results indicate that $Gd_2O_2CN_2$:Eu^{3+} is a promising red phosphor for white LEDs.

References

[1] C.M. Michail, G.P. Fountos, I.G. Valais, N.I. Kalyvas, P.F. Liaparinos, I.S. Kandarakis, and G.S. Panayiotakis, “Evaluation of the red emitting $Gd_2O_2CN_2$:Eu powder scintillator for use in indirect X-Ray digital mammography detectors”, IEEE Transactions on Nuclear Science , 2011, 58, 2503-2511.

[2] T.W. Chou, S. Mylswamy, R.S. Liu, S.Z. Chuang,“Eu substitution and particle size control of Y_2O_2S for the excitation by UV light emitting diodes”, Solid State Communications, 2005, 136, 205–209.

[3] V. Sivakumar, A. Lakshmanan, R.S. Kumar, S. Kalpana, R.S. Rani, and M.T. Jose, "Preparation and characterisation of yttrium based luminescence phosphors", Indian Journal of Pure &Applied Physics, 2012, 50, 123-128.

[4] Z.W. Zhang, L. Liu, S.T. Song, J.P. Zhang, D.J. Wang, "A novel red-emitting phosphors $Ca_9Bi(PO_4)_7:Eu^{3+}$ for near ultraviolet white light-emitting diodes", Current Applied Physics, 2015, 15, 248-252.

[5] Q.Y. Shao, H.J. Li, K.W. Wu, Y. Dong, J.Q. Jiang, "Photo luminescence studies of red-emitting NaEu(WO4)2 as a near-UV or blue convertible phosphor", Journal of Luminescence, 2009, 129, 879-883.

[6] V.P. Hedaoo, V.B. Bhatkar, S.K. Omanwar, "$PbCaB_2O_5$ doped with Eu^{3+}: A novel red emitting phosphor", Optical Materials, 2015, 45, 91-96.

[7] S. Neeraj, N. Kijima, A.K. Cheetham, Solid State Commun,2004,131, 65.

[8] C.F. Guo, T. Chen, L. Luan, W. Zhang, D.X. Huang, "Luminescent properties of $R_2(MoO_4)_3:Eu^{3+}$(R=La, Y, Gd) phosphors prepared by sol-gel process", Journal of Physics and Chemistry of Solid, 2008, 69, 1905-1911.

[9] J. Sindlinger, J. Glaser, H. Bettentrup, T. Jüstel, and H.-J. Meyer, "Synthesis of $Y_2O_2(CN_2)$ and luminescence properties of $Y_2O_2(CN_2)$:Eu", Z. Anorg. Allg. Chem., 2007, 633, 1686-1690.

[10] C.L. Lo, J.G. Duh, B.S. Chiou, C.C. Peng, L. Ozawa, "Synthesis of Eu^{3+}-activated yttrium oxysulfide red phosphor by flux fusion method", Materials Chemistry and Physics, 2001, 71, 179-189.

[11] Y. Hashimoto, M. Takahashi, S. Kikkawa, and F. Kanamaru, "Syntheses and Crystal Structures of Trigonal Rare-Earth Dioxymonocyanamides, $Ln_2O_2CN_2$ (Ln = Ce, Pr, Nd, Sm, Eu, Gd)", Journal of solid state chemistry, 1996, 125, 37–42.

[12] J. Holsä , R.-J. Lamminmäki , M. Lastusaari, P. Porcher, and E. Säilynoja, "Crystal field effect in RE -doped lanthanum oxycyanamide, $La_2O_2CN_2:RE^{3+}$(RE =$Pr^{3+}$and Eu^{3+}) ", Journal of Alloys and Compounds,1998, 275–277,402–406.

[13] X. M. Guo, W. S. Yu, X. T. Dong, J. X. Wang, Q. L. Ma, G. X. Liu, and M. Yang, "A Technique to Fabricate La2O2CN2:Tb3+ Nanofibers and Nanoribbons with the Same Morphologies as the Precursors", Eur. J. Inorg. Chem. 2015, 389–396.

[14] X. M. Guo, J. X. Wang, X. T. Dong, W. S. Yu, and G. X. Liu, "New strategy to achieve $La_2O_2CN_2:Eu^{3+}$ novel luminescent one-dimensional nanostructures" CrystEngComm, 2014, 16, 5409-5417.

[15] T. Takeda, N. Hatta, and S. Kikkawa, "Gel Nitridation Preparation and Luminescence Property of Eu-doped $RE_2O_2CN_2$ (RE =La and Gd) Phosphor", Chemistry Letters, 2006, 35, 988-989.

[16] Y. Hashimoto, M. Takahshi, S. Kikkawa, and F. Kanamaru, "Synthesis and Crystal Structure of a new compound, lanthanum dioxymonocyanamide ($La_2O_2CN_2$)", Journal of solid state chemistry, 1995, 114, 592-594.

[17] Y. Hashimoto, M. Takahashi, S. Kikkawa, and F. Kanamaru, "Syntheses of rare earth dioxymonocyanamides ($Ln_2O_2CN_2$, Ln=La, Ce, Pr, Nd, Sm, Eu, Gd)", Chemistry Letters, 1994, 1963-1966.

[18] P. Dorenbos, " The Eu^{3+} charge transfer energy and the relation with the band gap of compounds", Journal of luminescence, 2005, 111, 89-104.

[19] J. Y. Kuang, Y. L. Liu, and D. S. Yuan, “Preparation and characterization of $Y_2O_2S:Eu^{3+}$ phosphor via one-step solvothermal process”, Electrochemical and Solid-State Letters, 2005, 8(9), H72-H74.

[20] G. Blasse and B.C Grabmaier, Luminescent Materials, Springer, Berlin (1994).

[21] S.S. Yi, J.S. Bae, B.K. Moon, J.H. Jeong and J.H. Kim, “Crystallinity of Li-doped $Gd_2O_3:Eu^{3+}$ thin-film phosphors grown on Si (100) substrate”, Applied Physics Letters, 2005, 7(86), 1921-1923.

[22] G. Blasse, “Energy transfer in oxidic phosphors”, Physics Letters A, 1968, 28,444-445.

[23] X. L, L. Y. Yang, Q. L. Ma, J. Tian, X. T. Dong, “A novel strategy to synthesize Gd2O2S:Eu3+ luminescent nanobelts via inheriting the morphology of precursor”, Mater Electron, 2014, 25, 5388–5394.